Vol. A58 (1980) *ACTA PHYSICA POLONICA* No 6

# THE LAMELLAR MODEL OF FERROELECTRIC TGS-LIKE CRYSTALS AS AN ADEQUATE DESCRIPTION OF THEIR THERMAL EXPANSION AND OTHER PROPERTIES

By J. Stankowski and W. Malinowski

Institute of Molecular Physics, Polish Academy of Sciences, Poznań*

*(Received June 12, 1979; revised version received June 30, 1980)*

Measurements of the thermal expansion of TGS-like glycine crystals in the range $-30 < T-T_c < +20$ deg are reported. The expansion tensor components and their temperature dependence near $T_c$ are determined for TGSe, TGS and TGFB. The ferroelectric properties of TGS-like crystals are the most strongly affected by changes in dimension in the direction of the principal $\alpha_{33}$-axis of the thermal expansion tensor. A molecular model, explaining the mechanical and ferroelectric properties of TGS-like crystals, is discussed.

PACS numbers: 65.70.+y, 77.80.−e

## 1. *Introduction*

The thermal expansion ThE is an important thermodynamical property of crystals since it is the result of interactions and excitations of their constituent elements. Studies, concerning the ThE of crystals of the TGS group have been performed repeatedly [1–14] by various methods; however the results are still incomplete and, in some cases, even contradictory.

The first to study TGS were Ezhkova et al. [1], who applied the X-ray method, and Ganesan [2], who had recourse to the dilatometric method. Their measurements led to results which differed significantly as to the sign and nature of the temperature-dependence of the ThE coefficients in the directions of the Hoshino-Okaya-Pepinsky (HOP) *a* and *b*-axes. Shibuya et al. [3], in order to clarify these differences, carried out measurements by both methods in the two directions of TGS, and found that the results of Ganesan were correct for the *b*-direction and those of Ezhkova for the $a_{\mathrm{HOP}}$-direction.

ThE measurements were moreover performed for TGS in the directions of the HOP *a* and *b*-axes by Sirota et al. [4] using a quartz dilatometer, and by Tuktarova [5] by the

---

* Address: Instytut Fizyki Molekularnej PAN, Smoluchowskiego 17/19, 60-179 Poznań, Poland.

X-ray method. The latter work was aimed at determining the influence of X-irradiation on the temperature-dependence of ThE in TGS. Tuktarova found this dependence to be unaffected even if the X-ray dose was very considerable. The results of Refs [3–5] were, essentially, in agreement.

The work of Ezhkova and Ganesan led to the determination of the ThE tensor components for TGS crystal; however, with regard to the above-mentioned divergences, the results proved to be erroneous. The ThE tensor of TGS was determined anew by Telle [6], whose results in the directions of the various axes were in agreement with those reported in the above-cited papers.

Other studies on the ThE of TGS [7–10] dealt with the nature of the phase transition; their results concern the direction of the ferroelectric axis $\alpha_{22}$ only and, with the exception of the work of Imai [7], the narrow temperature region of about 1 deg near the transition point.

Imai performed a highly accurate study of one component, $\alpha_{22}$, of the ThE tensor of TGS.

The ThE of other crystals of the TGS group has not been investigated so thoroughly. For TGFB, measurements have been carried out by Warkusz et al. [11] and Varikash et al. [12]. The former determined the coefficients and components of the ThE by the X-ray method from the temperature-dependence of the lattice constants, and found a difference in ThE vs. temperature in the $a_{\mathrm{HOP}}$-direction by comparison with TGS crystal. The latter concentrated on the influence of irradiation on TGFB and did not determine the values of the ThE coefficients.

The ThE of TGSe has been studied by Varikash et al. [13] dilatometrically throughout a wide range of temperatures, and by Łukaszewicz [14] applying the X-ray method.

Our work, aimed at obtaining the values of the tensor for the three crystals TGS, TGSe and TGFB under identical conditions, as well as at a comparison of all the results hitherto available, proves that the lamellar model proposed by us provides the fullest explanation of the linear expansion and ferroelectricity of crystals of the TGS group.

## 2. *Results for the ThE tensors of TGSe, TGS and TGFB crystals*

ThE measurements were performed using an interference dilatometer [16]. The optical system provided for compensation of the changes in size of the instrument with changing temperature. During the measurements, the temperature was varied slowly and continuously, at a rate of about 0.3 deg/min. For each crystal, measurements were made in five directions i.e. in that of the ferroelectric axis and in four directions in the plane perpendicular thereto, namely, those of the HOP $a$ and $c$-axes and the $X$ and $Z$-axes of the Stankowski reference system [17], applied in EPR studies. The axes of the two systems of reference are shown in Fig. 1.

In all the crystals and directions, a singularity of the change in lenght vs. temperature was observed in the neighbourhood of the phase transition point. The relative changes in size of the crystals in the directions studied are shown in Fig. 2.

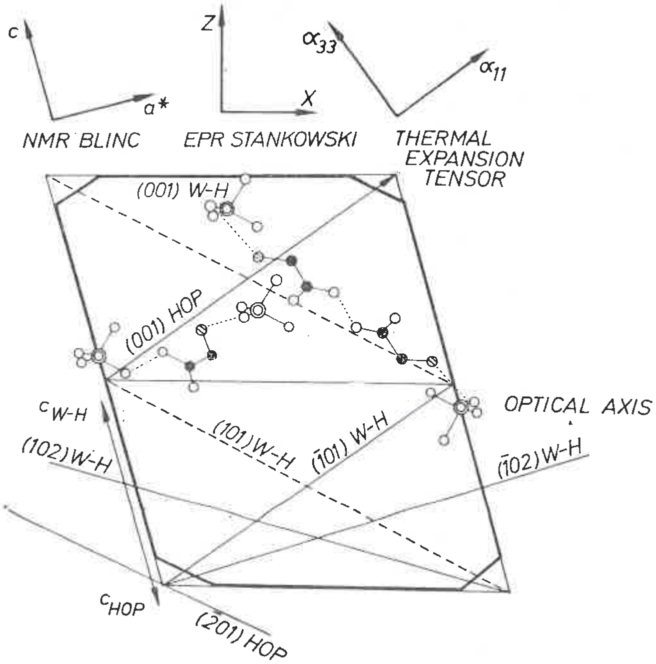

Fig. 1. Cross-section of TGS crystal in the (010) plane, and the orthogonal systems of reference applied in NMR and EPR work

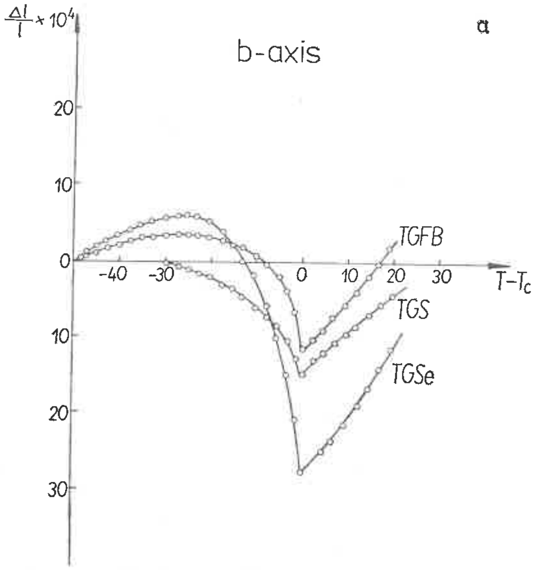

2a

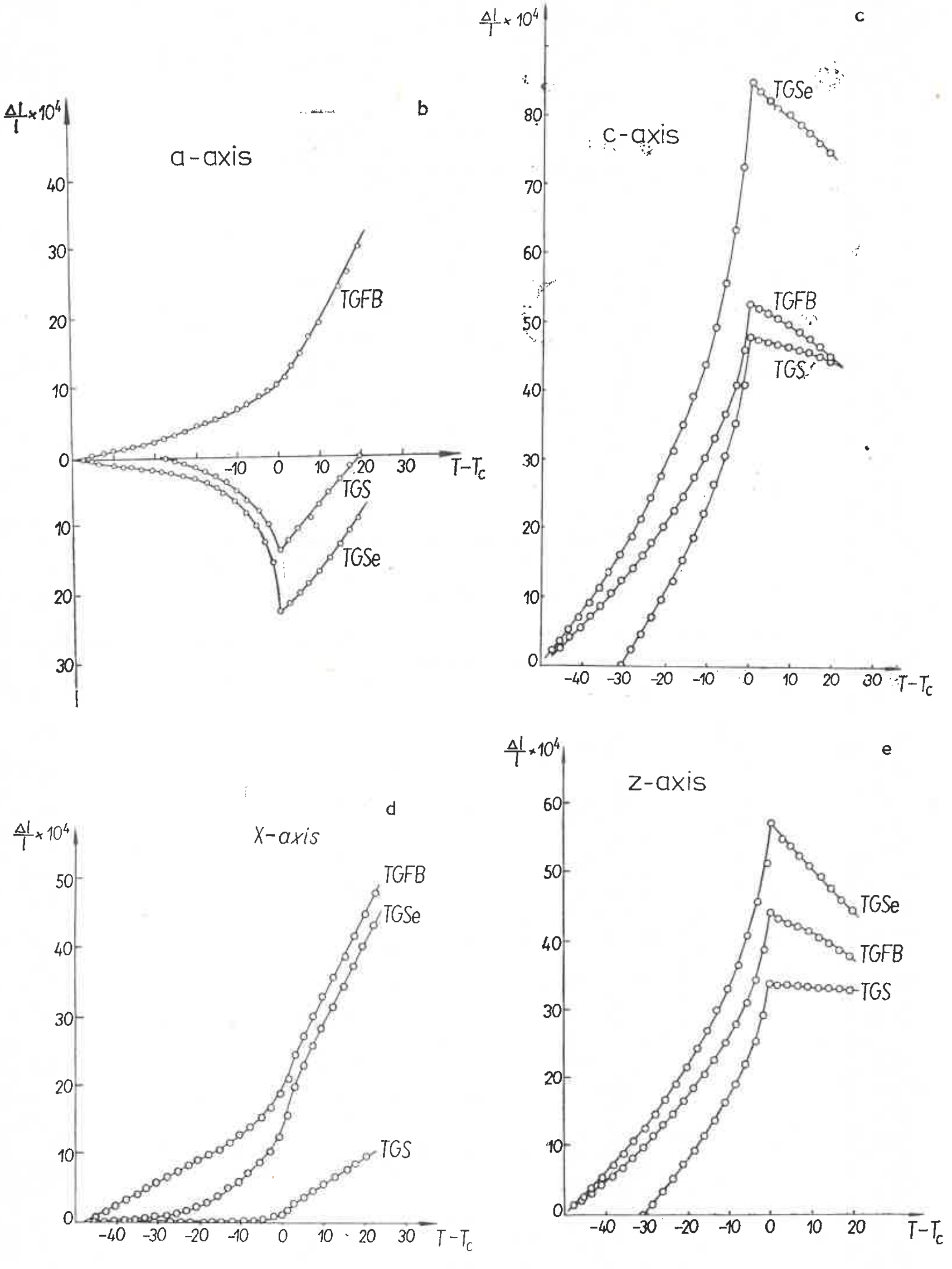

Fig. 2. Relative changes in the dimensions of TGS-like crystals measured, a) along the *b*-axis, b) along the $a_{\mathrm{HOP}}$-axis, c) along the $c_{\mathrm{HOP}}$-axis, d) along the *X*-axis, and e) along the *Z*-axis

TABLE I

Components of ThE tensor in *XYZ* coordinative frame and the principal values of ThE tensor for TGS

| $T$°C | $\alpha'_{11}$ | $\alpha'_{13}$ | $\alpha'_{33}$ | $\alpha_{11}$ | $\alpha_{22}$ | $\alpha_{33}$ | $\varphi$ |
|---|---|---|---|---|---|---|---|
| 19 | 0.18 | 4.50 | 6.92 | −2.08 | −1.30 | 9.18 | −27°25′ |
| 21.5 | 0.14 | 4.80 | 7.32 | −2.26 | −1.60 | 9.72 | −27°24′ |
| 24 | 0.04 | 5.24 | 7.76 | −2.60 | −1.90 | 10.42 | −27°13′ |
| 26.5 | 0.14 | 5.62 | 7.98 | −2.80 | −2.20 | 10.92 | −28°27′ |
| 29 | 0.20 | 6.34 | 8.32 | −3.26 | −2.70 | 11.78 | −29°19 |
| 31.5 | 0.32 | 7.08 | 8.76 | −3.70 | −3.20 | 12.78 | −30°24 |
| 34 | 0.22 | 9.26 | 9.30 | −4.66 | −3.80 | 14.18 | −31°24 |
| 36.5 | 0.18 | 9.86 | 10.18 | −5.00 | −4.40 | 15.36 | −31°43 |
| 39 | 0.38 | 9.82 | 11.16 | −5.44 | −5.30 | 16.96 | −31°23 |
| 41.5 | 0.62 | 11.22 | 12.46 | −6.14 | −6.40 | 19.22 | −32°55′ |
| 44 | 1.10 | 12.86 | 13.60 | −6.94 | −6.80 | 21.64 | −33°58 |
| 46.5 | 1.02 | 14.44 | 15.78 | −7.82 | −7.60 | 24.62 | −32°32 |
| 48 | 2.90 | 18.20 | 18.66 | −9.06 | −8.00 | 30.62 | −34°42 |
| 50 | 4.32 | −2.68 | −0.38 | 5.54 | 6.02 | −1.60 | −25°37 |
| 51.5 | 3.66 | −2.84 | −0.30 | 5.14 | 6.30 | −1.78 | −28°27 |
| 54 | 3.62 | −2.64 | −0.50 | 4.90 | 6.50 | −1.78 | −27°59 |
| 56.5 | 3.88 | −2.40 | −0.58 | 4.92 | 6.70 | −1.62 | −24°27 |
| 59 | 3.86 | −2.58 | −0.64 | 5.04 | 7.10 | −1.82 | −25°33 |
| 61.5 | 3.90 | −2.96 | −0.54 | 5.38 | 7.40 | −2.02 | −27°26 |
| 64 | 3.90 | −3.04 | −0.52 | 5.44 | 7.60 | −2.06 | −27°00 |
| 66.5 | 4.00 | −3.46 | −0.54 | 5.86 | 7.70 | −2.40 | −29°38 |
| 69 | 4.00 | −3.46 | −0.54 | 5.86 | 7.80 | −2.40 | −29°38 |

TABLE II

Components of ThE tensor in *XYZ* coordinative frame and the principal values of ThE tensor for TGFB

| $T$°C | $\alpha'_{11}$ | $\alpha'_{13}$ | $\alpha'_{33}$ | $\alpha_{11}$ | $\alpha_{22}$ | $\alpha_{33}$ | $\varphi$ |
|---|---|---|---|---|---|---|---|
| 33 | 3.36 | 2.48 | 4.86 | 1.52 | +1.40 | 6.70 | −37°25 |
| 35.5 | 3.14 | 2.36 | 5.18 | 1.58 | 1.30 | 6.74 | −34°41 |
| 38 | 3.28 | 2.38 | 5.70 | 1.82 | 1.20 | 7.16 | −32°28 |
| 40.5 | 3.14 | 2.28 | 6.06 | 1.90 | 0.60 | 7.30 | −29°19 |
| 43 | 3.14 | 2.42 | 6.38 | 1.84 | 0.40 | 7.68 | −29°54 |
| 45.5 | 3.18 | 2.60 | 6.60 | 1.78 | 0.00 | 8.00 | −29°40 |
| 48 | 3.44 | 2.54 | 6.92 | 2.10 | −0.20 | 8.26 | −28°13 |
| 50.5 | 3.36 | 2.60 | 7.52 | 2.12 | −0.80 | 8.76 | −26°20 |
| 53 | 3.44 | 2.76 | 7.88 | 2.12 | −1.20 | 9.20 | −26°24 |
| 55.5 | 4.32 | 3.20 | 8.04 | 2.48 | −1.60 | 9.88 | −30°05 |
| 58 | 4.48 | 3.52 | 9.00 | 2.56 | −2.40 | 10.92 | −29°21 |
| 60.5 | 4.68 | 3.88 | 9.84 | 2.60 | −3.60 | 11.92 | −29°49 |
| 63 | 5.26 | 4.54 | 10.50 | 2.64 | −4.40 | 13.12 | −31°59 |
| 65.6 | 5.94 | 4.60 | 12.28 | 3.54 | −6.40 | 14.70 | −28°17 |
| 68 | 7.84 | 5.70 | 13.46 | 4.30 | −8.20 | 17.00 | −32°07 |
| 70.5 | 8.66 | 6.94 | 18.34 | 5.04 | −12.40 | 21.96 | −28°27 |

TABLE II (continued)

| $T$°C | $\alpha'_{11}$ | $\alpha'_{13}$ | $\alpha'_{33}$ | $\alpha_{11}$ | $\alpha_{22}$ | $\alpha_{33}$ | $\varphi$ |
|---|---|---|---|---|---|---|---|
| 72 | 14.04 | 12.06 | 20.12 | 4.64 | −16.40 | 29.52 | −38°04 |
| 74 | 11.42 | −2.18 | −2.46 | 11.76 | +4.80 | −2.80 | −9°17 |
| 75.5 | 11.44 | −2.34 | −2.42 | 11.82 | 6.00 | −2.80 | −10°40 |
| 78 | 11.28 | −3.00 | −2.34 | 11.92 | 6.40 | −2.98 | −12°07 |
| 80.5 | 11.68 | −3.26 | −2.70 | 12.38 | 6.60 | −3.40 | −13°48 |
| 83 | 11.82 | −3.94 | −3.46 | 12.78 | 7.00 | −4.42 | −14°22 |
| 85.5 | 12.04 | −4.08 | −3.64 | 12.04 | 7.20 | −4.64 | −14°15 |
| 88 | 12.30 | −5.02 | −3.48 | 13.76 | 7.50 | −4.94 | −17°46 |
| 90.5 | 12.28 | −4.16 | −3.92 | 13.28 | 7.60 | −4.92 | −14°24 |
| 93 | 12.42 | −4.42 | −4.08 | 13.52 | 7.80 | −5.18 | −15°55 |

TABLE III

Components of ThE tensor in *XYZ* coordinative frame and the principal values of ThE tensor for TGSe

| $T$°C | $\alpha'_{11}$ | $\alpha'_{13}$ | $\alpha'_{33}$ | $\alpha_{11}$ | $\alpha_{22}$ | $\alpha_{33}$ | $\varphi$ |
|---|---|---|---|---|---|---|---|
| −18 | 0.46 | 3.82 | 6.32 | −1.38 | 2.80 | 8.20 | −27°00 |
| −15.5 | 0.70 | 4.20 | 6.88 | −1.42 | 2.60 | 9.00 | −27°10 |
| −13 | 0.70 | 4.20 | 7.40 | −1.32 | 2.20 | 9.42 | −26°17 |
| −10.5 | 0.80 | 4.22 | 7.80 | −1.34 | 2.00 | 9.94 | −26°11 |
| −8 | 1.46 | 5.02 | 8.40 | −1.18 | 1.20 | 11.04 | −28°20 |
| −5.5 | 1.34 | 4.92 | 8.78 | −1.10 | 0.06 | 11.22 | −27°33 |
| −3 | 2.14 | 5.72 | 9.40 | −1.18 | −0.80 | 12.72 | −30°45 |
| −0.5 | 2.64 | 6.58 | 9.82 | −1.26 | −2.00 | 12.72 | −31°19 |
| 2 | 3.26 | 7.98 | 10.48 | −1.88 | −4.40 | 15.62 | −33°10 |
| 4.5 | 4.14 | 10.42 | 11.10 | −3.36 | −7.40 | 18.60 | −36°14 |
| 7 | 4.44 | 11.62 | 11.64 | −4.12 | −8.80 | 20.20 | −37°36 |
| 9.5 | 4.90 | 13.28 | 12.30 | −5.18 | −10.60 | 22.38 | −38°47 |
| 12 | 5.52 | 15.40 | 14.08 | −6.18 | −13.60 | 25.78 | −38°46 |
| 14.5 | 6.88 | 19.00 | 16.72 | −7.82 | −17.00 | 31.42 | −38°16 |
| 17 | 8.62 | 23.46 | 19.44 | −10.04 | −19.80 | 38.10 | −39°30 |
| 19.5 | 12.34 | 28.82 | 21.84 | −12.12 | −22.10 | 46.30 | −41°41 |
| 21 | 18.22 | 39.46 | 24.68 | −28.12 | −24.60 | 76.02 | −44°52 |
| 23 | 10.84 | 0.48 | −7.50 | 10.86 | 5.20 | −7.52 | 1°30 |
| 24.5 | 11.22 | 0.02 | −5.94 | 11.22 | 5.40 | −5.94 | 0°04 |
| 27 | 11.44 | −0.10 | −6.12 | 11.44 | 6.40 | −6.12 | −1°40 |
| 29.5 | 11.66 | −0.38 | −6.24 | 11.66 | 6.50 | −6.24 | −2°47 |
| 32 | 12.04 | −0.60 | −6.32 | 12.06 | 6.70 | −6.34 | −2°08 |
| 34.5 | 12.26 | −0.46 | −6.46 | 12.28 | 6.80 | −6.48 | −2°36 |
| 37 | 12.22 | −0.56 | −6.54 | 12.24 | 6.80 | −6.56 | −2°18 |
| 39.5 | 12.46 | −0.58 | −6.64 | 12.48 | 6.90 | −6.66 | −2°16 |
| 42 | 12.44 | −0.42 | −6.68 | 12.44 | 6.90 | −6.68 | −2°45 |

The expansion measurements in five directions permitted the determination of the ThE tensor components by the least squares method. Tables I–III give the values of the tensor components at various temperatures in the system of axes *XYZ* as well as in that of principal axes of the ThE tensor $\hat{\alpha}$. Due to the crystal symmetry, the principal axis $\alpha_{22}$ coincides with the ferroelectric axis. The angle $\varphi$ defines the position of the ThE axis $\alpha_{33}$ in the plane perpendicular to the ferroelectric axis, with respect to the Stankowski *Z*-axis.

The orientation of the axes of the ThE tensor and the shape of the temperature dependence of its components were found to be similar for all the crystals of the TGS group. However, there is a difference between TGSe, TGS and TGFB with regard to the principal $\alpha_{11}$-axis, i.e. the direction in which the dilativity is the least: have, the tensor component is negative in TGSe and TGS and positive (though small) for TGFB.

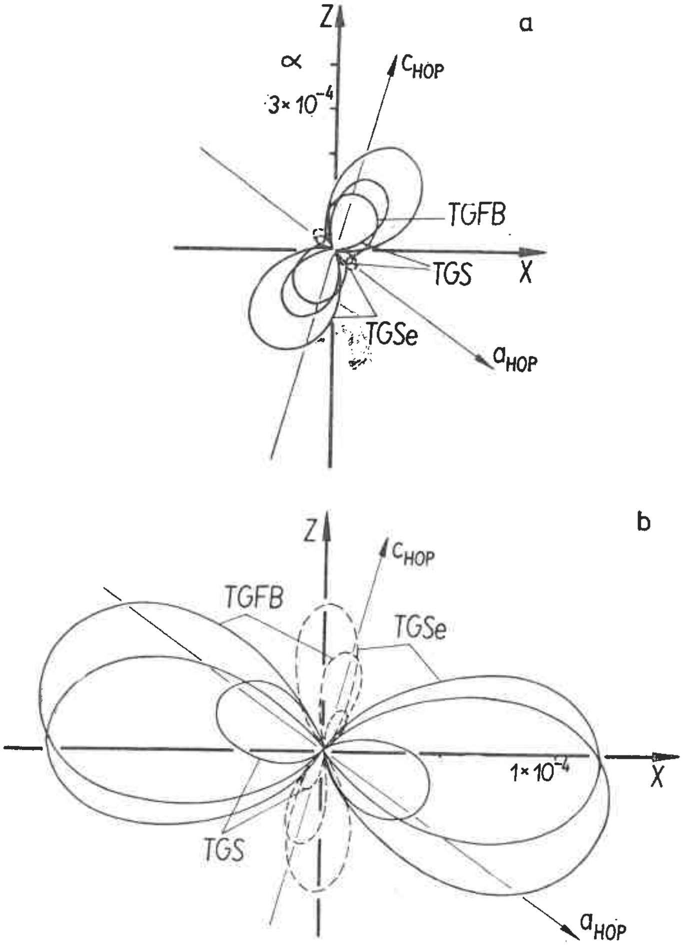

Fig. 3. Polar dependence of the linear dilativity coefficient in the (010) plane: a) ferroelectric phase, b) paraelectric phase

The values of the ThE tensor components thus determined permit the calculation of the expansion coefficient value in any given direction. Fig. 3 shows polar graphs of the ThE coefficients in the plane (010) of the crystals. This plane contains the direction of the $\alpha_{33}$-axis, in which the expansion is maximal. In the ferroelectric phase it corresponds, in a good approximation, with the direction perpendicular to the HOP *a*-axis, and the change in size of the crystals, are by one order of magnitude greater in the direction than in that of the $\alpha_{11}$-axis.

Our results for TGS crystal are in agreement with those reported by Telle [6] and Shibuya [3]. Our ThE coefficients for the direction of the ferroelectric axes are, in the immediate lower-temperature neighbourhood of the transition point, slightly larger as to their absolute value than those reported by others.

For TGFB, our values are in good agreement with those of Warkusz et al. [11] as to their values and the shape of their temperature-dependence.

For TGSe, the shape of the temperature-dependence found by us is in principle concordant with that of Varikash [13]. However, the ThE coefficients in the phase transition point are not so large as to absolute value as those of others. Also, we found a negative $\alpha$-value for the paraelectric phase in the HOP *c*-direction, as for the other TGS-like crystals.

## 3. *Discussion of the results*

### 3.1. Thermodynamical theory

To Janovec [18, 19] is due a general relation between the ThE coefficients and other thermodynamical parameters describing the state of the crystal. For TGS, as the symmetry changes from $2/m$ to 2, the relations of $\alpha_\mu$ with the elasticity constant and pressure-coefficient of the Curie point $\gamma_\mu = \partial T_c/\partial\sigma_\mu$ take the form:

$$\alpha_\mu^{TE} = \frac{c^{\sigma E}}{T}\gamma_\mu + \alpha_\mu^{tE}, \tag{1}$$

$$S_{\mu\nu}^{TE} = \alpha_\mu^{TE}\gamma_\nu + S_{\mu\nu}^{tE}, \tag{2}$$

where $\mu, \nu = 1, 2, 3, 5$.

From the relation (1) given above the values of $\gamma$-coefficients based on our ThE measurements and literature data on specific heat [42, 43] were calculated. For TGSe and TGS the experimental values of $\gamma_\mu$ measured by Stankowska et al. [19] in the principal directions of the ThE tensors were found to be extremal, whereas in the case of TGFB only $\gamma_2$ was determined. The both sets of data are given in Table IV. They show that the axes of tensors $\hat{\alpha}$ and $\hat{\gamma}$ do coincide and that the Curie point displacement due to hydrostatic pressure are in very good agreement with the data of Samara [20] and Stankowski [21] except for that calculated for TGS. The observed discrepancy in $\gamma$ for TGS according to Pippard-Janovec theory points out the inconsistency of ThE and specific heat data. Nevertheless, good agreement between the values of coefficients $\gamma$ given by Samara and measured by Stankowska in the principal directions of our ThE tensor as well as selfconsistency of ThE data are highly encouraging. We cannot explain the observed discrepancy but it seems that our

TABLE IV

Values of $\gamma$-coefficient measured by Stankowska [21] in $XYZ$ coordinative frame and calculated as slopes of $\alpha_\mu$ vs. $c_p/T \times 10$ milideg/MPa

| Crystal | Measured | | | $\sum_1^3 \gamma_\mu$ | Calculated |
|---|---|---|---|---|---|
| | $\gamma_1$ | $\gamma_2$ | $\gamma_3$ | | |
| TGSe | $-18.6$ | $-9.4$ | $+31.6$ | $+3.6$ | $+3.6$ |
| TGS | $-9.2$ | $-9.3$ | $+21.1$ | $+2.6$ | $+8.6$ |
| TGFB | | $-12.4$ | | | $+2.3$ |

ThE data can be taken as a basis for further discussion also in case of TGS. The properties of TGS-like crystals and the nature of their phase transition are the subject of discussion since the strong isotopic effect in TGSe changing the transition from second order in TGSe to first order in DTGSe [22–25] with a typical Merz hysteresis loop causes us to proceed forthwith to the molecular mechanism of ferroelectricity in TGS.

### 3.2. Molecular theory

The ThE coefficient is related with anharmonicity in the mutual interaction of elements constituting the crystal:

$$\alpha = \frac{K}{r_0} \frac{b}{a^2} \tag{3}$$

with: $K$ — Boltzmann's constant; $r_0$ — the distance at equilibrium; $a$, $b$ — constants of the equation for the force $f = -a\bar{x} + b\bar{x}^2$ dependent on the mean deviation $\bar{x}$ from the equilibrium position.

The analysis of the linear ThE coefficient tensor enables us to draw conclusions regarding the bonding directions and lattice planes in the crystal. In crystal with lamellar structure, the THE coefficient $\alpha_{\parallel}$ is small in the bond plane and is maximal ($\alpha_{\perp}$) in the direction perpendicular to the packing density plane. No linear expansion or hardly any is exhibited by molecular crystal in the hydrogen bond direction [26]. The molecular "membrane" mechanism [27] also permits the explanation of the negative linear ThE coefficient in the packing density plane.

A highly interesting molecular approach to ferroelectricity in TGS has been proposed by Zaslavskii et al. [28], who applied the theory of weakly nonlinearly interacting vibrations, explaining instabilities in charged particle beams in accelerator [28] to explain the instability of the TGS lattice below $T_c$. They considered collective harmonic vibrations of the $SO_4$ ions and localized anharmonic vibrations of glycine GI. Within the approximation of moderate anharmonicity of interaction with the negatively charged end of $SO_4^-$, the GI molecule can undergo a permanent deviation from the (010) plane leading directly to the emergence of the ferroelectric phase. The instability condition requires that:

$$\left(\frac{\alpha}{\varepsilon}\right)^{1/2} \gg 1, \tag{4}$$

where $\alpha$ is a dimensionless anharmonicity parameter and $\varepsilon$ the parameter of interaction between the two (the delocalized and localized) modes. The model under consideration is corroborated by the splitting of 63 $\mathrm{cm}^{-1}$ vibrations below $T_c$ observed in TGS crystal by Shabanov et al. [30] and Cervenka et al. [31]. The results of Ref. [31] moreover determine the magnitude of the deviation from equilibrium; on the soft mode theory of Thomas [32], a mechanism of this kind leads to a transition with displacement.

### 3.3. The lamellar structural model for TGS-like crystals

The unit cell of monoclinic crystals of the TGS-group has been determined by Wood and Holden [33] and, using a different method, by Hoshino, Okaya and Pepinsky [34]. The mutual disposition of the cells and of the frames (axes) of reference corresponding to them are shown in Fig. 1. The $b$ axis is shared by the two systems of reference; its direction coincides with that of spontaneous polarization of the crystal. The directions of the $c$ axes of both systems are the same albeit with opposite sense, so that $c_{\mathrm{W-H}} = -c_{\mathrm{HOP}}$. Fig. 1. (upper part) moreover shows the orientation of the axes of the two most commonly used orthogonal systems of reference: that of Blinc [35] in NMR studies, and that of Stankowski [17] in EPR work.

The results reported here for the ThE tensor $\hat{\alpha}$ have shown the direction of greatest expansion of the crystals (that of the principal axis $\alpha_3$ of $\hat{\alpha}$) to be approximately perpendicular to the direction of the axis $a_{\mathrm{HOP}}$. The third of the orthogonal systems of reference shown in Fig. 1 is that of the principal axes of the ThE tensor. The similar disposition of the principal axes of the other tensors describing the properties of TGS-like crystals [36] led us to search for other distinguishable structural elements corresponding to these directions, and provided the basis for proposing the Stankowski lamellar model of the structure of crystals belonging to the family under discussion [15].

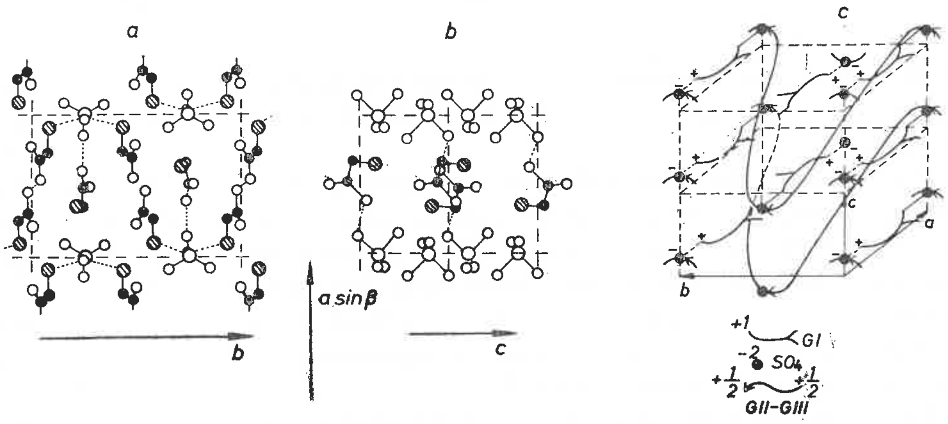

Fig. 4. Lamellar model of TGS crystal: a) projection of the $SO_4^-$-GII-GIII-SO- chain on the (010) plane, b) unit cell cross-sections $y = 1/4b$ and $y = 3/4b$ in which the inter-chain bonds $GI^+ — SO_4^-$ lie, c) spatial view of TGS crystal

The model is based on the assumption that the planar glycines GII and GIII are bonded by a strong hydrogen bridge, denoted as "short". This gives rise to a prolate dimeric ion, having the structure of a glycine dimer at whose ends are situated $NH_3$ groups, performing rotation at room temperature. The effective charge of either end of the ion amounts to $+\frac{1}{2}e_0$. Two such dimer ions are bonded by one negative charge of the $SO_4^{2-}$ ion localized on the oxygen atom $O_2$ (according to HOP notation).

The TGS crystal structure is a system of molecular chains, formed of $SO_4^{2-}$ ions and dimer ions $(GII\text{–}GIII)^{1+}$. The chains form densely packed planes, parallel to the ferroelectric axis and located close to the HOP $(\bar{2}01)$ plane (see Fig. 1).

The glycine molecule GI is hydrogen bonded by way of an oxygen atom O to the oxygen $O_1$ of $SO_4$ (after HOP notation). The $NH_3$ group of GI rotating at room temperature has a charge of $+1\ e_0$, which compensates the other negative charge of the $SO_4^{2-}$ group localized on the oxygens $O_3$ and $O_4$.

Neighbouring chains are connected by way of interaction between the $NH_3$ group of GI and the $SO_4$ group. The molecular chains, constituting the structural elements of the crystal within the framework of Stankowski's model, are shown in Fig. 4. The glycine GI, weakly bonded by $NH_3^+$ to $SO_4^-$ in the rigid chain, has considerable freedom of motion, leading to the large electric permittivity in the Curie point and the large spontaneous polarisation below $T_c$.

Independently of geometrical considerations, further facts justifying the preceding choice of structural elements for crystals of the TGS family are to be found in the results of optical and radiospectroscopic studies. Raman [31] and IR [30] spectral studies have proved the existence of a phonon mode, shared by GII and GIII in both phases, weakly dependent on temperature, and not subject to change in the phase transition point. A similar behaviour is exhibited by the temperature-dependence of quadrupole splitting at nuclear resonance of deuterons of the rotating $NH_3$ groups of GII and GIII [35]. Studies of electron resonance for chromium ion admixture $Cr^{3+}$ have shown the orientation of the principal deformation direction of the nearest neighbourhood of $Cr^{3+}$ not to vary with temperature, even at transition through $T_c$; now, as we know [37, 38], this neighbourhood consists of GII, GIII and two $SO_4$ groups.

The preceding shows that the molecular chains, providing the basis for the lamellar structure of TGS-like crystals are, in fact, a stable element of their structure.

## 4. *Final remarks*

The interaction between various molecular fragments of the lamellar model fall in the categories: intra-chain interactions, defined by ionic interaction between the dimer ion (GII–GIII) and $SO_4$ ions, and inter-chain interactions defined by ionic bonds $GI^+\text{—}SO_4^-$ and covalent interaction between the chains. Information on the intra-chain interactions is provided by electron resonance studies of admixture ions. The coordination surroundings of an admixture $Cr^{3+}$ ion comprises two $SO_4$ groups, and molecules GII and GIII. The crystal field deformation in the coordination surroundings of $Cr^{3+}$ as measured by the fine structure parameter $D$ of the spin Hamiltonian is the least in TGFB, larger in TGS and the largest in TGSe.

The temperature-dependence $\frac{dD}{dT}$ in the paraelectric phase of these crystals is given by the ratio (0 : 2 : 4), signifying that the paramagnetic complex is the most strongly bound to the rest of the crystal in TGSe and the least strongly in TGFB.

Inter-chain interaction depends on the packing density. The latter is the least in TGSe, and the greatest in TGFB. The unit cell volumes twenty deg below $T_c$ amount to 674.6; 645.2 and 633.7 Å$^3$, respectively. The sequence of transition points $T_c^{\mathrm{TGSe}}$ (295 K) < < $T_c^{\mathrm{TGS}}$ (322 K) < $T_c^{\mathrm{TGFB}}$ (345 K), which reflects the magnitude of interaction between the elements of the lattice, points to inter-chain interaction as the essential factor of the transition to the ferroelectric state.

Experiments applying one-dimensional pressure have shown that distention of the TGS-type lattice along the HOP $a$-axis favours the ferroelectric state, whereas compression in the same direction favours the paraelectric state of the crystal [19, 39, 40]. Weakening of the $\mathrm{GI^+}$—$\mathrm{SO_4^-}$ bond causes a deviation of the positively charged $\mathrm{NH_3}$ group out of the (010) plane as well as a change in orientation of the whole $\mathrm{O_2C}$—C — skeleton of the GI molecule (Fig. 5). Qualitatively the process is described by the theory of Zaslavskii et al.

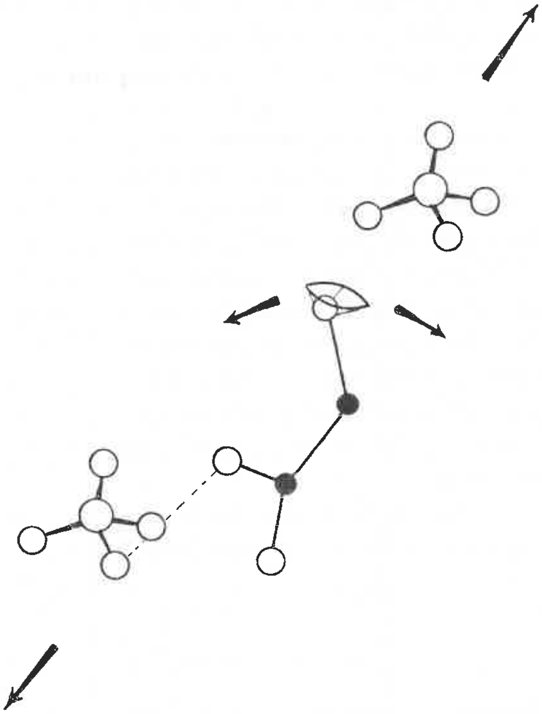

Fig. 5. Distention of the $\mathrm{GI^+}$ — $\mathrm{SO_4}$ bond leads to instability of the paraelectric structure

[28], since as the inter-chain bond GI—$SO_4$ becomes weaker the parameter $\varepsilon$ of Eq. (4) decreases, leading to the condition for instability of the lattice.

As shown by the NMR work of Hoffmann et al. [42] for deuterized TGS, the $ND_3$ group is involved in librational motion and, moreover, there occurs a jumpwise change in position of the glycine I skeleton in $T_c$. Now if the temperature variation effect of the deuterium spectrum in $ND_3$ were wholly related with molecular flipping, the deviation of GI out of the (010) plane could be related to probabilities of deviation in inverse directions; the average position would then be given by the following expression:

$$\langle\beta\rangle = \frac{p_+\beta_+ + p_-\beta_-}{p_+p_-}, \tag{5}$$

where $p_+, p_-$ are the tilting probabilities of GI into either of the possible positions. For the paraelectric phase $p_+ = p_-$, so that

$$\langle\beta\rangle = (\beta_+ + \beta_-)/2.$$

Below the Curie point

$$p_+ = 1 + a(T_c - T)^{1/2}, \quad p_- = 1 - a(T_c - T)^{1/2},$$

whence we obtain:

$$\langle\beta\rangle = \frac{\beta_+ + \beta_-}{2} + \frac{\beta_+ - \beta_-}{2}\,\frac{(T_c - T)^{1/2}}{T_c}.$$

In order to check this relationship we proceeded to a comparison with the quadrupole splitting vs. angle dependence, found by Hoffmann et al. for deuterized TGS. Fig. 6 shows

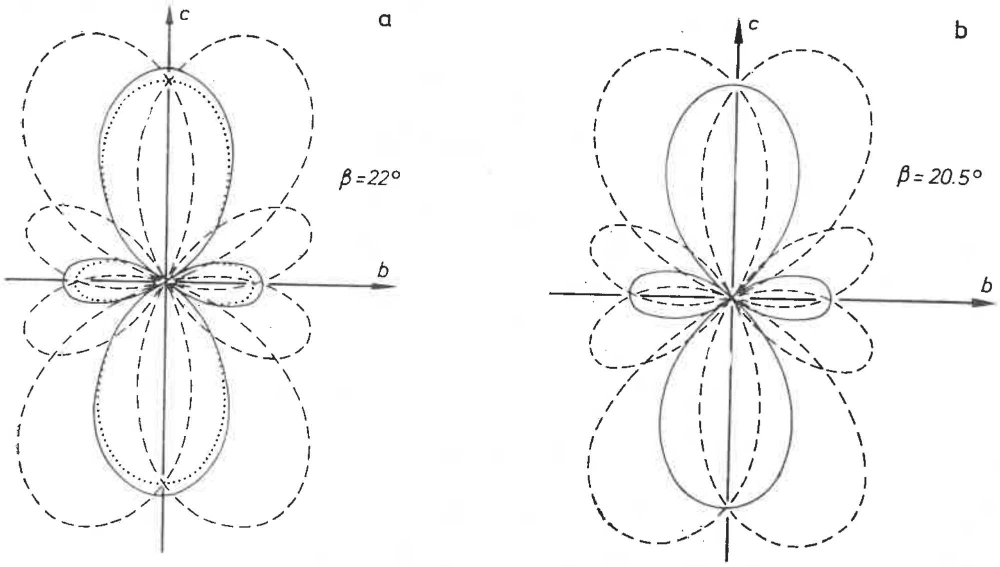

Fig. 6. Two ways of averaging the quadrupole splitting tensor 2D of the $NH_3$ group in DTGS: a) flipping by an angle of $\beta = 22°$, b) flipping by $\beta = 20.5°$ and steric deviation of $NH_3^+$ by an angle $\alpha = 1.5°$

the $Q$-tensor averaged in the HOP $bc$-plane on the assumption of $|\beta_+| = |\beta_-| = 22.5°$ as the summary value of the deviation angle of $Q_{zz}$ from the (010) plane. One finds that the averaged value exceeds that obtained in the paraelectric state. A good fit is obtained only if $|\beta_\pm| = 20.5°$ signifying that in addition to orientational averaging in $T_c$ there occurs a jumpwise change in orientation by an angle of 1.5° of the GI skeleton as a whole. This result is a proof of the complex nature of the phase transition, consisting in an averaging of the angle $\beta$ and a jumpwise deviation of GI as a whole by an angle $\alpha$.

The polarisation of the TGS unit cell originates in the dipole moment due to displacement of $NH_3^+$ from the (010) plane, rather than in the polarity of the GI molecule. We suggested this earlier, and it is hence obvious that the magnitude 3D of the electric moment of glycine consists of the 2.3 D contribution from $NH_3^+$ displacement and only 0.6 D resulted by the projection of the dipole moment of $NH_3$ onto the ferroelectric axis $b$.

The orientation of one of the GI's determines that of the other GI's in neighbouring chains. This accounts for the strong unipolarity of TGS crystals, since stabilization of one GI in polar position polarizes the whole lenght of the chain of GI molecules into the direction of the HOP $a$ axis.

The presence of a chain structure, consisting of dimer ions GII—GIII and $SO_4$ groups, and flipping motion of GI, provide the explanation for the thermal expansion of crystals of the TGS type. By way of the chain structure, the expansions in the directions of the axes $\alpha_{33}$ and $\alpha_{22}$ are related with each other directly. An increase in dimension in the $\alpha_{22}$-direction causes a decrease in the $\alpha_{33}$-direction. The change in position of the GI skeleton on transition from the paraelectric to the ferroelectric phase, and the deviation of $NH_3$ with decreasing temperature, cause an increase in dimension in the direction of the ferroelectric axis of the crystal — in that of the $\alpha_{22}$-axis of the ThE tensor. This is related with interaction of the $NH_3$ group and the oxygens $O_3$ and $O_4$ of $SO_4^{2-}$ (in HOP notation). Hence the negative expansion coefficient value for this direction and the positive value for the $\alpha_{33}$-axis direction. Flipping of GI fully explains the large expansion coefficient for $\alpha_{33}$ near $T_c$, since the crystal has to undergo extension in this direction in order that the angle $\beta$ can attain its average, $\langle\beta\rangle = 0$. The large difference between the coefficients for $\alpha_{22}$ and $\alpha_{33}$ is due to superposition of the effects of normal, positive expansion and those originating in the chain structure. This is supported by the change in sign of the coefficient for $\alpha_{22}$ occuring in the ferroelectric phase at about 30 deg below $T_c$. In the lower temperature region the expansion coefficient in the direction of the $\alpha_{22}$-axis takes positive values, as the changes in dimension due to deviation of $NH_3$ cease to predominate over normal, positive expansion.

The authors wish to thank Doc. dr habilit. J. Stankowska for her kindness in providing the crystals and for her part in the study of the $\gamma$-tensor.

## REFERENCES

[1] Z. I. Ezhkova, G. S. Zhdanov, M. M. Umanskii, *Kristallografiya* **4**, 249 (1959).
[2] S. Ganesan, *Acta Cryst.* **15**, 81 (1962).
[3] I. Shibuya, S. Hoshino, *Japan J. Appl. Phys.* **1** (5), 249 (1962).

[4] N. M. Sirota, V. M. Varikash, *Kristallografiya i fazovye perekhody*, Izv. AN BSSR, Minsk 1962.

[5] L. S. Tuktarova, *Kristallografiya* **10**, 432 (1965).

[6] F. Telle, *Compt. Rend.* (Paris) **262B**, 1087 (1966).

[7] K. Imai, *J. Phys. Soc. Japan* **43** (4), 1320 (1977).

[8] K. Deguchi, E. Nakamura, *Phys. Lett.* **60A** (4), 351 (1977).

[9] S. Gilespie, H. K. Schurmann, J. D. Gunton, T. Michalisin, *Solid State Commun.* **15**, 1753 (1974).

[10] K. H. Ehses, H. Meister, C. Zeyen, *Ferroelectrics* (in press).

[11] F. Warkusz, K. Łukaszewicz, *Bull. Acad. Pol. Sci. Ser. Sci. Chim.* **21**, 9, 669 (1973).

[12] V. M. Varikash, T. A. Zarembovskaya, Zh. P. Lagutina, *Kristallografiya* **17**, 873 (1972).

[13] V. M. Varikash, I. V. Agarkov, *Dokl. AN BSSR* **10**, 461 (1966).

[14] K. Łukaszewicz, *Fizyka i chemia ciała stałego*; Ed. B. Staliński, Ossolineum (1977).

[15] J. Stankowski, *Ferroelectrics* **20**, 109 (1978).

[16] W. Malinowski, Proc. of Conf. Electronics and Non-linear Optics EKON 76, Poznań 1976.

[17] J. Stankowski, *Acta Phys. Pol.* **33**, 387 (1968).

[18] V. Janovec, *J. Chem. Phys.* **45**, 1847 (1966).

[19] J. Stankowska, I. Polovinko, J. Stankowski, *Ferroelectrics*, in press.

[20] G. A. Samara, *Advances in High Pressure Research*, Acad. Proc., *J. Phys. Soc. Japan* **28**, 399 (1970).

[21] J. Stankowski, A. Gałęzewski, S. Waplak, U. Gruszczyńska, H. Gierszal, *Ferroelectrics* **6**, 209 (1974).

[22] E. V. Peshnikov, *Fiz. Tverd. Tela* **14**, 1597 (1972).

[23] K. Gesi, *J. Phys. Soc. Japan* **41**, 565 (1976).

[24] L. A. Shuvalov, A. I. Baranov, A. M. Shirokov, V. P. Konstantinova, *Ferroelectrics* **14**, 669 (1976).

[25] A. Czarnecka, J. Stankowska, *Acta Phys. Pol.* **A53**, 155 (1978).

[26] A. I. Kitajgorodski, *Kryształy molekularne*, PWN 1976 (in Polish).

[27] S. I. Novikova, *Thermal Expansion of Solid State*, Izd. "Nauka", Moskva 1974.

[28] G. M. Zaslavski, V. F. Shabanov, K. S. Aleksandrov, I. P. Aleksandrova, *Zh. Eksp. Teor. Fiz.* **72**, 602 (1977).

[29] G. M. Zaslavski, B. V. Chirkov, *Usp. Fiz. Nauk* **105**, 3 (1977).

[30] V. F. Shabanov, A. V. Sorokin, *Izv. Akad. Nauk* SSSR **33**, 734 (1977).

[31] P. O. Cervenka, A. D. Prasad Rao, S. P. S. Porto, *Ferroelectrics* **11**, 511 (1976).

[32] H. Thomas, *Structural Phase Transitions and Soft Modes*, Universitets Forleget (1971).

[33] E. A. Wood, N. Holden, *Acta Cryst.* **10**, 145 (1957).

[34] S. Hoshino, Y. Okaya, R. Pepinsky, *Phys. Rev.* **115**, 2, 323 (1959).

[35] R. Blinc, M. Pintar, I. Zupanic, *J. Phys. Chem. Solids* **28**, 405 (1967).

[36] J. Helwig, J. Albers, *Phys. Status Solidi* (a) **7**, 151 (1971).

[37] J. Stankowski, S. Waplak, V. A. Yurin, *Phys. Status Solidi* **22**, K41 (1974).

[38] S. Waplak, T. Terlecka, M. Krupski, *Acta Phys. Pol.* **A50**, 71 (1976).

[39] K. Gesi, K. Ozawa, *J. Phys. Soc. Japan* **40**, 599 (1976).

[40] F. Gilletta, *Phys. Status Solidi* **59**, K103 (1973).

[41] S. K. Hoffmann, L. S. Szczepaniak, J. Stankowski, *J. Magn. Resonance* (in press).

[42] B. A. Strukov, *Fiz. Tverd. Tela* **6**, 2862 (1964).

[43] B. A. Strukov, S. A. Taraskin, V. A. Koncik, *Zh. Eksp. Teor. Fiz.* **51**, 1037 (1966); B. A. Strukov, S. A. Taraskin, V. M. Varikash, *Fiz. Tverd. Tela* **10**, 1836 (1968).